

Long-Distance Coupling and Energy Transfer between Exciton States in Magnetically Controlled Microcavities

Maciej Ściesiek,¹ Krzysztof Sawicki,¹ Wojciech Pacuski,¹ Kamil Sobczak,²
Tomasz Kazimierczuk,¹ Andrzej Golnik,¹ and Jan Suffczyński^{1,*}

¹*Institute of Experimental Physics, Faculty of Physics,
University of Warsaw, Pasteura St. 5, 02-093 Warsaw, Poland*

²*Biological and Chemical Research Centre, University of
Warsaw, Żwirki i Wigury St. 101, 02-089 Warsaw, Poland*

(Dated: June 8, 2021)

Abstract

Coupling of quantum emitters in a semiconductor relies, generally, on short-range dipole-dipole or electronic exchange type interactions. Consistently, energy transfer between exciton states, that is, electron-hole pairs bound by Coulomb interaction, is limited to distances of the order of 10 nm. Here, we demonstrate polariton-mediated coupling and energy transfer between excitonic states over a distance exceeding 2 μm . We accomplish this by coupling quantum well-confined excitons through the delocalized mode of two coupled optical microcavities. Use of magnetically doped quantum wells enables us to tune the confined exciton energy by the magnetic field and in this way to control the spatial direction of the transfer. Such controlled, long-distance interaction between coherently coupled quantum emitters opens possibilities of a scalable implementation of quantum networks and quantum simulators based on solid-state, multi-cavity systems.

Keywords: exciton, optical microcavity, polariton, semimagnetic semiconductor, energy transfer

*Electronic address: Jan.Suffczynski@fuw.edu.pl

Introduction

Energy transfer between quantum emitters, such as excitons in a semiconductor, relies on a coupling through short-range dipole-dipole (Förster)[1] or electronic exchange (Dexter)[2] type interactions. The distance of these interactions is typically of the order of 10 nm in III-V or II-VI semiconductors.[3, 4] As shown in the pioneering work by Agranovich *et al.*,[5] the spatial range of energy transfer in semiconductor systems can be enhanced utilizing the light-matter coupling effects. In the strong light-matter coupling regime the exciton and the optical mode of the microcavity exchange energy in a reversible way, which leads to a superposition of their wave functions and the emergence of a new eigenstate called an exciton-polariton [6–12]. When several excitonic states are strongly coupled to a common optical mode, their wave functions hybridize enabling their mutual coupling. In this way polariton-mediated transfer of energy between distant excitons is possible. The energy transfer remains efficient as long as the strong coupling conditions and hybridization of the initial and final excitonic states of the process are maintained.[13] As such, it enables an enhancement of the energy transfer range by orders of magnitude with respect to the Förster limit.[13–17]

In this work, we report on magnetic field controlled, polariton-mediated energy transfer between 2D exciton states over a distance as large as $2.15 \mu\text{m}$. We achieve this in structures containing (Cd,Zn)Te and (Cd,Mn,Zn)Te quantum wells strongly coupled to the modes of two coupled microcavities separated by a semi-transparent Bragg mirror (see Figure 1a). In such a system the polariton wave function contains a component originating from exciton in two different quantum wells and from the two coupled optical modes. As a result, the polariton relaxation from a level with a dominant contribution by the exciton from one quantum well to a level with a dominant contribution by the exciton from another well is accompanied by a change in the spatial position of the exciton. In this way, the polariton relaxation is accompanied by energy transfer between different, separated in space, quantum wells. Doping of the quantum wells in one of the microcavities with a small amount of Mn^{2+} ions enhances the exciton Zeeman splitting in magnetic field due to the *s,p-d* exchange interaction between the extended band states and the localized spins of the Mn^{2+} ions (see Figure 1b).[20] To maximize exciton splittings we choose the Faraday geometry with magnetic field applied along the sample growth direction, thus parallel to the quantization axis. In consequence, we are able to tune the energy of the excitons in the Mn-doped

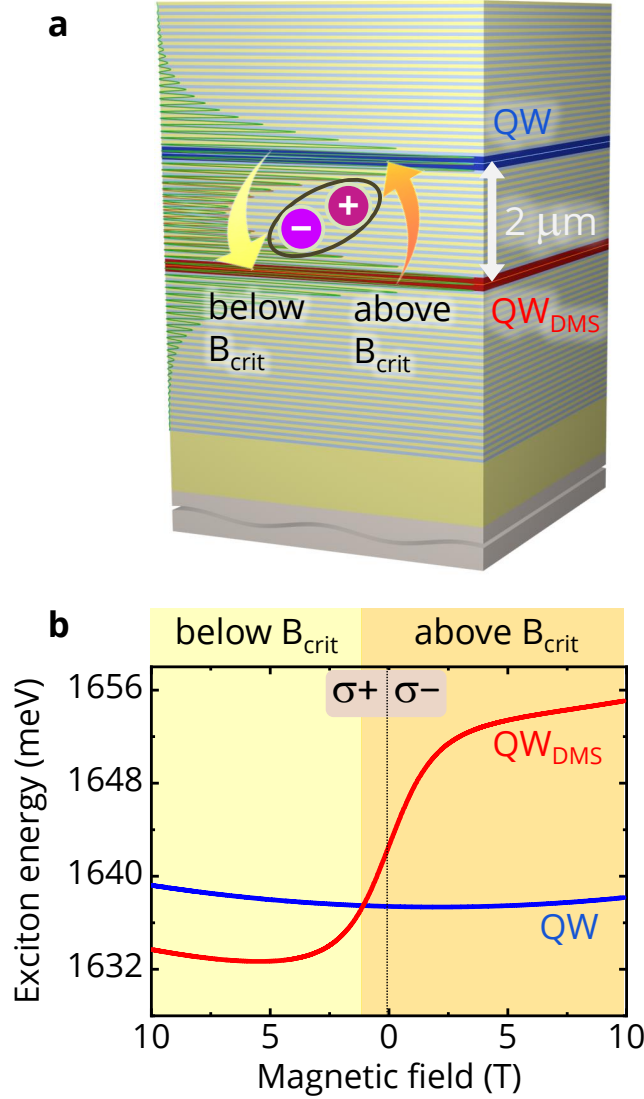


FIG. 1: **Schematic view of magnetic field controlled, polariton-mediated energy transfer between exciton states over 2 μm .** **a** Coupled microcavity structure hosting spatially delocalized symmetric (C_S) and antisymmetric (C_{AS}) optical modes (respective distributions of the squared electric field shown). Three non-magnetic quantum wells (QW) are placed in the upper and three magnetically doped quantum wells (QW_{DMS}) are placed in the lower microcavity. Under strong coupling conditions a four-level polariton system emerges inducing hybridization of excitons in the QW_{DMS} and QW . Long-distance transfer of energy between the QW and QW_{DMS} is possible thanks to the optical mode mediated coupling of the initial and final excitonic states of the process. **b** Energy levels of the QW (blue line) and QW_{DMS} (red line) as a function of the magnetic field. The energy of the excitons in the QW_{DMS} can be tuned below or above the energy of the excitons in the QW ; the crossing occurs at B_{crit} . Below B_{crit} , exciton density transfer assisted by energy relaxation occurs predominantly from the QW to the QW_{DMS} , while above B_{crit} the transfer direction is reversed.

quantum well (QW_{DMS}) below or above the energy of the excitons in the non-magnetic quantum well (QW) using a magnetic field.[21] Since the exciton density transfer between the wells is assisted by energy relaxation, by adjustment of the relative energy order of the excitons in the QW_{DMS} and QW one gains control of the direction of the transfer, as schematically shown in Figure 1a.

Results

Four-level polaritonic system

As shown in Figure 2a-c, three 10 nm wide non-magnetic (Cd,Zn)Te quantum wells and three 12 nm wide, Mn^{2+} doped (semimagnetic) (Cd,Mn,Zn)Te quantum wells are, as intended, embedded in the centre of the upper and lower microcavity, respectively. Incorporation of the Mn^{2+} ions only in the QW_{DMS} is confirmed by the Transmission Electron Microscopy images shown in Figure 2d-e.

In order to prove evidence for the formation of a four-level polaritonic system in the studied sample, in Figure 3 we show emission spectra of the structure resolved in in-plane photon momentum space k_{\parallel} . The spectra are registered at consecutive positions on the sample along the direction of the microcavity thickness gradient, i.e. as a function of the detuning between the coupled, symmetric (C_{S}) and antisymmetric (C_{AS}), optical modes of the structure and the QW and QW_{DMS} excitons. For an even number of Bragg pairs separating the microcavities, as in the present case, the C_{S} mode is *higher* in energy than the C_{AS} one.

The case of a large negative detuning between the excitons and microcavity modes is shown in Figure 3a. Exciton-photon mixing is negligible here, and individual components contributing to the four-level polaritonic system are clearly distinguished. The approximately parabolic dispersion identifies the C_{S} and C_{AS} modes. The QW transition with a negligible dispersion is seen at around 1640 meV, while the QW_{DMS} one occurs at 1645 meV. Excitation energy below the bandgap energy of any layer of the structure except the QW and QW_{DMS} ensures that the excitation penetrates both microcavities. The absorption of the quantum wells in the upper microcavity is below 10%, which means that carriers are generated in the quantum wells in the upper and lower microcavities with comparable efficiency.

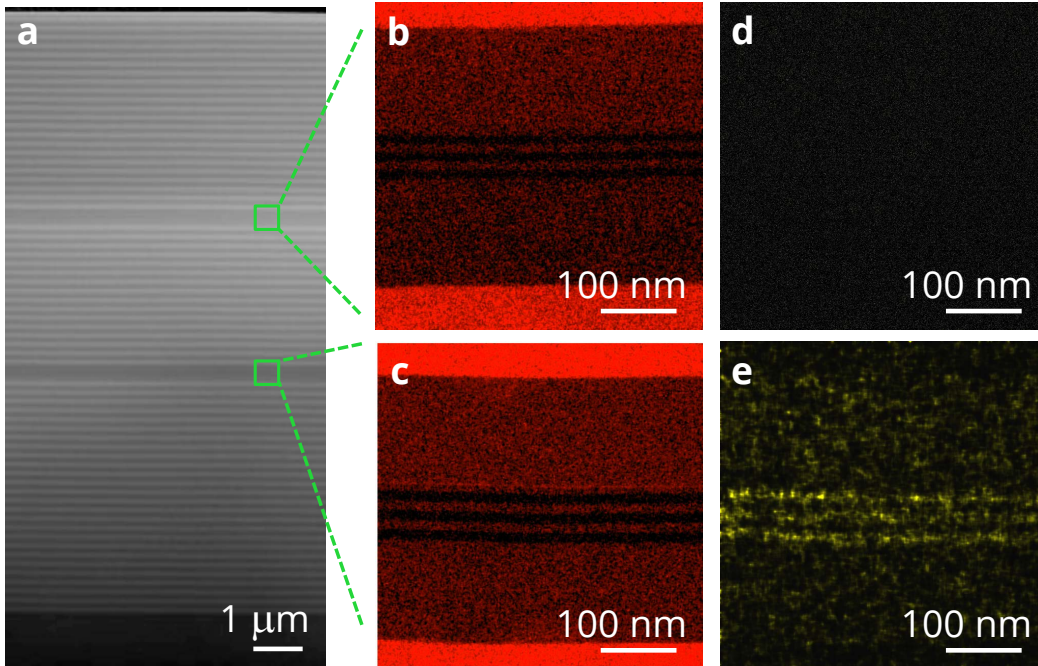


FIG. 2: **Transmission Electron Microscopy images of double coupled microcavities cross-section.** **a** The structure comprises two (Cd,Zn,Mg)Te microcavities coupled by a semi-transparent Bragg mirror. Three (Cd,Zn)Te and three (Cd,Mn,Zn)Te quantum wells are embedded in the upper and lower microcavities, respectively, as confirmed by the Energy-Dispersive X-ray spectroscopy investigations of spatial distribution of Mg atoms (panels **b** and **c**) and Mn atoms (panels **d** and **e**) in the sample cross-section.

Emission from the QW_{DMS} is vanishingly weak, however, due to its filtering by the stopbands of the middle and upper Bragg mirrors. When the coupled modes approach the excitonic levels, anticrossing is observed (see Figure 3b), which testifies to strong light-matter coupling conditions. Figure 3c shows the case of modes-excitons resonance. In contrast to the case shown in Figure 3a, all four emitting levels exhibit a clear dependence on k_{\parallel} , proving a non-negligible contribution by the photonic part to each state of the four-level polaritonic system.

In order to describe the observed polariton dispersion quantitatively, we introduce the Hamiltonian H (Eq. 1) representing a four coupled oscillator model [22–24]. The Hamiltonian H written in the basis of the exciton states QW and QW_{DMS} , with mode M localized in the upper and mode M_{DMS} localized in the lower microcavity, takes the form:

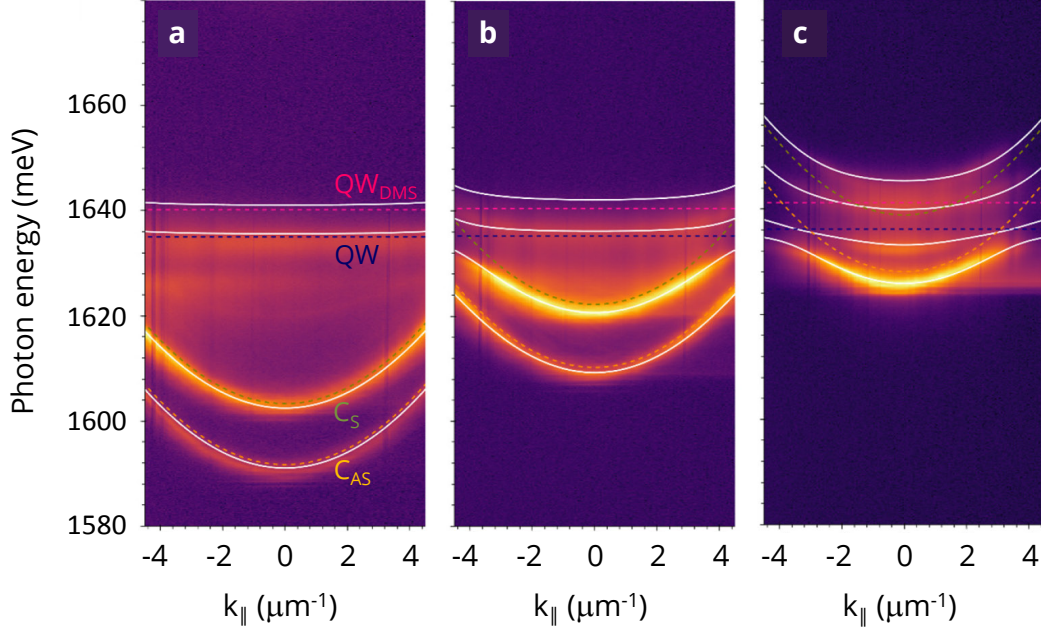


FIG. 3: **Formation of a four-level polariton system in double coupled microcavities with quantum wells.** Emission spectra resolved in in-plane photon momentum k_{\parallel} (shown on a logarithmic intensity scale). Dotted lines represent the uncoupled exciton states in the QW and QW_{DMS} , as well as the optical modes C_S and C_{AS} delocalized spatially over the two coupled microcavities. Solid lines represent polariton levels calculated as eigenvalues of the Hamiltonian H (Eq. 1). Detuning between the optical modes and exciton levels increases from **a** to **c**.

$$H = \begin{pmatrix} QW & \Omega/2 & 0 & 0 \\ \Omega/2 & M & \kappa/2 & 0 \\ 0 & \kappa/2 & M_{DMS} & \Omega_{DMS}/2 \\ 0 & 0 & \Omega_{DMS}/2 & QW_{DMS} \end{pmatrix}. \quad (1)$$

Off-diagonal elements of the matrix represent couplings in the system, κ describes the strength of the interaction between the (degenerate) M and M_{DMS} giving rise to the emergence of the C_S and C_{AS} optical modes [22, 25–27] delocalized spatially over the two microcavities (the respective squared electric field distributions for the C_S and C_{AS} modes are shown in Figure 1a), Ω is the coupling constant between the QW exciton and the mode M of the upper microcavity and Ω_{DMS} represents the coupling between the QW_{DMS} exciton and the M_{DMS} mode of the lower microcavity. Direct coupling of the excitons with the optical mode confined in the adjacent microcavity is neglected [22–24].

Fitting the energies obtained from diagonalization of the Hamiltonian H to the energies of the optical transitions reported in Figure 3 determines the value of κ to be 13 meV. Such a value is, in fact, expected for a microcavity separation of 16 Distributed Bragg Reflector (DBR) pairs,[27, 28] as in the present case. The vacuum Rabi splitting Ω for the QW exciton is (10.0 ± 0.4) meV, and Ω_{DMS} for the QW_{DMS} exciton is (12.5 ± 0.4) meV. In simulations, only the bare level energies are changed by detuning, while the coupling constants remain fixed (they change by less than 10% when changing the position on a $7 \text{ mm} \times 20 \text{ mm}$ sample). In terms of the splitting energy per quantum well, the values obtained are consistent with previous reports on II-VI polariton systems [8, 29–32].

We note that the coupling constants are of the same order as the energy separation between the QW and QW_{DMS} excitons. This means that the coupling with the delocalized optical modes of the structure indeed ensures hybridization of the QW and QW_{DMS} states, being a prerequisite for efficient polariton-mediated energy transfer between the quantum wells.

In previous studies, the magnetic field applied in Faraday geometry enabled lowering of the polariton condensation threshold[18] or, when applied in the Voigt geometry, controlling of the polariton condensate propagation in single microcavities.[19] Here, we demonstrate photon-mediated exciton interaction and energy transfer between the macroscopically distant quantum wells in double microcavity structure and use the magnetic field as a mean to control of the transfer direction.

Photon-mediated interaction between magnetic and non-magnetic exciton

Figure 4 shows the emission spectra resolved in circular polarization, registered as a function of magnetic field for consecutive detunings between the microcavity modes and quantum well excitons decreasing from panel a to d. Corresponding Hopfield coefficients [33] determined from the diagonalization of the Hamiltonian H (Eq. 1) are shown below the spectra (note the labels run from 1 to 4 in order of increasing level energy). Below we analyze the emission energy and intensity of the dependencies observed in the experiment.

The non-resonant case, where the coupled modes are far detuned to higher energy with respect to the quantum well excitons (around 20 meV at $B = 0$ T), is shown in Figure 4a. In this case, the observed emission arises predominantly from the exciton confined in the QW ,

as indicated by only a slight change in the emission energy and intensity upon application of the magnetic field (at $B = 10$ T σ^- intensity I^{σ^-} is higher than the σ^+ intensity I^{σ^+} by a factor of $\lesssim 2$). Such a small splitting, as well as only weak (below 30%) and negative polarization of the emission ($= (I^{\sigma^+} - I^{\sigma^-}) / (I^{\sigma^+} + I^{\sigma^-})$) is expected in the case of a non-magnetic quantum well, since only linear Zeeman splitting (excitonic g-factor of 0.7, consistent with Ref. 34) and diamagnetic shift ($\gamma = 0.018$), both of relatively small magnitude, affect the exciton energy $E_{QW}^{\sigma\pm}(B)$:

$$E_{QW}^{\sigma\pm}(B) = E_{QW}(B = 0) \pm g\mu_B B + \gamma B^2 \quad (2)$$

In the case of the QW_{DMS} , the exciton energy $E_{QW_{DMS}}^{\sigma\pm}(B)$ varies much more upon application of magnetic field due to an additional contribution coming from the $s,p-d$ exchange interaction between the exciton spin and the localized $5/2$ spins of the Mn^{2+} ions:

$$E_{QW_{DMS}}^{\sigma\pm}(B) = E_{QW_{DMS}}(B = 0) \mp \frac{E_{sat}}{2} B_{5/2} \left(\frac{\frac{5}{2} g_{Mn} \mu_B B}{k_B T_{eff}} \right) \pm g\mu_B B + \gamma B^2. \quad (3)$$

In Eq. 3 the term $E_{sat} = x_{Mn}(N_0\alpha - N_0\beta)S_0$ represents exciton giant Zeeman splitting at saturation, defined by the Mn dopant concentration x_{Mn} , the $s-d$ and $p-d$ exchange integrals $N_0\alpha = 0.22$ eV and $N_0\beta = -0.88$ eV, respectively for electrons and holes, and $S_0 = 2.12$ being the effective spin of the Mn^{2+} ion in (Cd,Mn)/Te.[35] The $B_{5/2}$ is the modified Brillouin function[35] with parameters: Mn^{2+} ion Landé factor $g_{Mn} = 2$, Bohr magneton μ_B , effective temperature of the Mn spins $T_{eff} = 2.3$ K, and the Boltzmann constant k_B .

It is worth to note, that crossing of the QW and QW_{DMS} exciton levels occurring at around $B_{crit} = 0.8$ T at σ^+ polarization in Figure 4a does not affect the energy of the emission. This indicates that when the mode is far detuned from the excitons, no interaction between excitons in the QW and QW_{DMS} occurs. The negligible hybridization of the QW and QW_{DMS} states in the non-resonant case is reflected by a sharp exchange of the QW and QW_{DMS} components in the polariton states 1 and 2 when the magnetic field passes B_{crit} (see the Hopfield coefficients for levels 1 and 2 in Figure 4a). The emission from the QW_{DMS} in the non-resonant case is filtered out by the middle and upper DBRs. Thus despite being excited by the laser, it is not manifested in the spectrum. In the non-resonant case, the emission spectral width is just the linewidth of the QW confined neutral exciton transition. It is larger than the radiative lifetime defined limit due to a sample structural disorder. An additional broadening of the emission towards lower energy seen in Figure 4a is attributed to a presence of transition of charged exciton[36, 37] confined in the QW .

The resonant case, where either the C_{AS} or C_S mode is tuned to the close spectral vicinity of the quantum well levels, is shown in Figure 4b or 4c, respectively. The spectra reveal an anticrossing of the polariton states for which a contribution from the QW and QW_{DMS} exciton dominates (they are, respectively, levels 1 and 2 in Figure 4b and levels 2 and 3 in Figure 4c). The anticrossing occurs at polarization $\sigma+$ at $B_{crit} = 0.8$ T, where the uncoupled QW and QW_{DMS} exciton levels cross, proving the photon-mediated interaction between the macroscopically distant, magnetic and non-magnetic, excitons. The Hopfield coefficients confirm enhanced hybridization of the QW and QW_{DMS} excitons in the resonant case. In the resonant case, the emission spectral width is the average of the QW exciton and the mode linewidths weighted by the respective contributions of the two components to the emitting state. In the following discussion by conditions "below B_{crit} " we mean $B > B_{crit}$ in $\sigma+$ polarization, while by "above B_{crit} " we mean the remaining field range and polarization of the signal (i.e., $B < B_{crit}$ in $\sigma+$ and $B > 0$ T in $\sigma-$ polarization).

Magnetic field controlled, polariton-mediated energy transfer over a macroscopic distance

Let us now consider the emission intensity dependences, starting from the resonant ("*transfer on*") case shown in Figure 4b. Below B_{crit} , the dominant contribution to level 1 comes from the exciton confined in the QW_{DMS} , while the dominant contribution to level 2 comes from the exciton confined in the QW . Quantum wells in both microcavities are excited with comparable intensity, and the QW_{DMS} emission is not as efficiently filtered out by the DBRs stopband as it was in the non-resonant case. Thus, if there were no exciton density transfer between the QW and QW_{DMS} one would expect a comparable emission intensity from levels 1 and 2. This is clearly not the case: the emission occurs mostly from the lowest in energy, polariton level 1. The observed enhancement of the population of level 1 and depletion of the population of level 2 reflects the efficient relaxation of the polaritons to level 1 from level 2. This points towards efficient exciton density transfer from the QW placed in the upper microcavity to the QW_{DMS} placed in the lower microcavity, 2.15 μm away. The observed behaviour, in particular the depletion of the polariton level 2, cannot result from intrawell spin relaxation of the exciton in the QW , since its spin polarization is weak (see Figure 4a) and it is not affected by a superposition with the optical mode (at

least below the polariton condensation density, as in the present case).[38–40]

Exciton density transfer between the QW and QW_{DMS} does not require exciton spin relaxation. It is assisted, however, by its energy relaxation. The energy difference between the QW and QW_{DMS} excitons is relatively small (up to 5 meV, depending on the magnetic field), which facilitates its efficient dissipation by acoustic phonons and ensures high exciton density transfer rates [41]. Measurements of time-resolved micro-photoluminescence from the cleaved edge of the sample indicate that the lifetime of the exciton in either the QW or QW_{DMS} is around 200 ps (not shown). We thus state that the transfer time is much smaller than this value, in the range of tens of ps or shorter.

In turn, above B_{crit} in Figure 4b the contribution to the lowest polariton level 1 from the QW exciton dominates over the contribution from the QW_{DMS} exciton. A dominant population of level 1 above B_{crit} indicates that the direction of the transfer is reversed and the exciton density shifts from the QW_{DMS} to the QW . Here, due to the large splitting of the QW_{DMS} exciton for $B > 0$ T, an additional contribution to the depletion of the $\sigma-$ polarized exciton in the QW_{DMS} exciton appears, resulting from spin and energy exciton relaxation within the QW_{DMS} [20]. The excitation, kept constant during the magnetic field dependent measurements, is linearly polarized and non-resonant, so that it does not introduce any imbalance between $\sigma+$ and $\sigma-$ populations of the photocreated excitons.

The energy and intensity dependences of the resonant ("*transfer on*") case presented in Figure 4c are similar to the case in Figure 4b. Excitons contributing to polaritons on the most populated level 2 originate predominantly either from the QW (for B below B_{crit}) or the QW_{DMS} (for B above B_{crit}). Comparable dependences in Figure 4b and Figure 4c point towards their similar interpretation and indicate that both coupled modes C_S and C_{AS} mediate the energy transfer between the quantum wells with comparable efficiency. Such a result is consistent with comparable intensities of the electric field associated with C_S and C_{AS} at the centres of the microcavities, as seen in Figure 1a. Analysis of the Hopfield coefficients in Figure 4c reveals that feeding of the polariton levels indeed occurs through the quantum well excitons, as polariton level 2, of strongly excitonic character, is much more populated than the lowest, but mostly photonic in nature, level 1. Consistently, emission from the level 1 in $\sigma+$ polarization, where a net exciton component is present (see the Hopfield coefficients) is stronger than in $\sigma-$ polarization, where the exciton content to level 1 is negligible.

Finally, Figure 4d shows that when the optical modes are far detuned to lower energy with respect to the quantum well excitons ("transfer off" case), the ordinary crossing of exciton energy levels of quantum wells occurs. This indicates that the photon-mediated interaction and energy transfer between the QW and QW_{DMS} exciton states have been turned off again. Also in this case, a net exciton content results in enhancement of the $\sigma+$ polarized with respect to $\sigma-$ polarized emission of the level 2.

Discussion

Photon-mediated hybridization of excitonic states and enhanced energy transfer efficiency over distances of the order of 100 nm have been studied so far in microcavities with embedded layers of organic molecules [13–16, 42–45] or hybrid structures involving perovskite or two-dimensional transition metal dichalcogenides layers [46–50]. Very recently, use of a hybrid organic-inorganic coupled microcavity enabled the energy transfer on a distance reaching 1.5 μm [17].

A long-distance, spin-dependent interaction and polariton-mediated energy transfer between quantum emitters demonstrated in the present work are promising for deterministic designing of novel photonic devices such as, e.g., bosonic Josephson junctions [51–53], so far limited to disordered polaritonic systems. Formation of spatially delocalized polaritons in a coupled multi-cavity structure and the possibility of their manipulation by a magnetic field makes the presented system useful for studies and implementation in the recently intensively developing areas of quantum polariton networks [54], quantum simulators [55] and production of hyper-entangled photons with a strongly reduced noise background [56].

The present study has been performed in a linear regime, where interactions between the polaritons are negligible due to their small density. An exciting extension of this work would be a study of the presented four-level polaritonic system to the high excitation limit, where stimulated scattering in a non-linear regime induces such effects as the polariton Bose-Einstein condensation. Such a study should not only answer the question whether the condensate can boost a long-distance energy transfer in a semiconductor, but it should also enable observation of new phenomena, such as magnetic field tunable polariton parametric scattering between polariton branches or switchable, multiple wavelength polariton lasing. Enhancement of optical nonlinearities thanks to the exciton hybridization should enable an

ultra-low threshold for lasing.

Conclusions

We have accomplished magnetic field controlled coupling and energy transfer between semiconductor quantum wells over a distance exceeding $2 \mu\text{m}$. The distant interaction is ensured by the strong coupling of the excitons to a common optical mode delocalized over the two coupled microcavities. The magnetic field enables control of the strength of the coupling and the energy order of the semimagnetic quantum well exciton with respect to the non-magnetic quantum well exciton. This makes possible control of the direction of the polariton-mediated energy transfer by an external magnetic field, which is promising for magnetic field controlled routing of the excitation in a semiconductor. The multilevel system presented is attractive for further studies of nonlinear polariton effects and for a wide range of applications in optoelectronics and quantum information science.

Methods

Sample

The structures are grown by molecular beam epitaxy on a ZnTe buffer layer deposited on a (100) oriented GaAs substrate, with real-time monitoring of the thickness of the layers by *in situ* reflectivity during around 12 hours of growth. The structure contains two (Cd,Zn,Mg)Te $3\lambda/2$ microcavities ($n_{cav} = 2.7$ at $\lambda = 750 \text{ nm}$). The microcavities are sandwiched between and separated by DBRs made of 30, 16 and 28.5 pairs of alternating refractive index layers in the case of the lower, the middle and the upper mirrors, respectively (see Figure 2a). High ($n_{high} = 2.95$ at 750 nm) and low ($n_{low} = 2.4$ at 750 nm) refractive index layers are made of (Cd,Zn,Mg)Te with, respectively, 10% and 50% Mg content. Both microcavities are of wedge type, which results in a gradient of the mode energy of 10.5 meV/mm , as deduced from reflectivity spatial mapping. At every point on the sample the microcavities share the same thickness, which ensures a maximum degree of coupling between their optical modes. The quality factor of the microcavities deduced from the coupled modes linewidth observed in reflectivity exceeds 2000. The energy gradient of a quantum well confined exciton amounts to around 0.6 meV/mm . The concentration of the manganese in QW_{DMS} is determined to

0.8% by fitting a modified Brillouin function[35] to the QW_{DMS} exciton shift in the magnetic field.

Experiment

Photoluminescence is non-resonantly *cw* excited at 1.81 eV ($\lambda_{exc} = 685$ nm). For far-field distribution of the emission measurements, the sample is placed inside a helium-flow cryostat at 8 K. The laser beam is focused to a 1-2 μm diameter spot at the sample surface using a microscope objective (numerical aperture of 0.7). The in-plane photon momentum k_{\parallel} is registered in the range from $-4.5 \mu\text{m}^{-1}$ to $4.5 \mu\text{m}^{-1}$ by imaging the Fourier plane of the microscope objective on the entrance slit of the spectrometer. For magnetic field dependent measurements, the sample is placed inside a pumped helium cryostat at 1.8 K equipped with a superconducting split-coil magnet producing a magnetic field of up to 10 T. The measurements are performed in the Faraday configuration. The combination of a quarter-wave plate and a linear polarizer allows for the detection of two circular polarizations. The laser beam is focused to a 0.1 mm diameter spot at the sample surface using a 500 mm focal length lens. The lens is mounted on an automated XY translation stage, which enables spatial mapping of the photoluminescence with a step of 0.01 mm. The range of registered k_{\parallel} vectors is limited to $0.42 \mu\text{m}^{-1}$ in this case. A CCD camera coupled to a grating spectrometer serves as a detector (0.1 meV of the overall spectral setup resolution).

Transmission Electron Microscopy (TEM) observations are conducted on a FEI Talos F200X microscope operating at 200 kV. The measurements are performed in Scanning TEM (STEM) mode using a high-angle annular dark-field detector and Energy-dispersive X-ray spectroscopy on a Bruker BD4 spectrometer. Cross-sectional TEM specimens are prepared by a standard method of mechanical pre-thinning followed by Ar ion milling.

TMM Simulations

The spatial distribution of the electric field in the structure shown in Figure 1a is calculated using the transfer matrix method. Complex refractive indices of the layers are assumed following the literature [57].

Data availability

The data that support the findings of this study are available from the corresponding author upon reasonable request.

Competing interests

The authors declare no competing interests.

Acknowledgments

We gratefully acknowledge sample preparation for the TEM measurements by Jolanta Borysiuk (deceased), and we dedicate this work to her. This work was partially supported by the Polish National Science Centre under projects DEC-2013/10/E/ST3/00215 and DEC-2017/25/N/ST3/00465. The research was carried out with the use of CePT, CeZaMat and NLTK infrastructures financed by the European Union - the European Regional Development Fund within the Operational Programme "Innovative economy" for 2007-2013.

Author contributions statement

M.Ś was involved in all steps of this work. J.S. was involved in all steps of this work apart from the sample growth. W.P. epitaxially grew the samples. K.S. and T.K participated in optical measurements. A.G. participated in design of the studies and interpretation of the results. K.So. performed TEM measurements. J.S wrote and all authors reviewed the manuscript.

-
- [1] T. Förster, *Zwischenmolekulare Energiewanderung und Fluoreszenz*, *Annalen der Physik* **437**, 55 (1948).
- [2] D. L. Dexter, *A Theory of Sensitized Luminescence in Solids*, *The Journal of Chemical Physics* **21**, 836 (1953).

- [3] W. Heimbrodt, L. Gridneva, M. Happ, N. Hoffmann, M. Rabe, and F. Henneberger, *Tunneling and energy transfer in ZnSe-based semimagnetic double quantum wells*, Physical Review B **58**, 1162 (1998).
- [4] G. Itskos, G. Heliotis, P. G. Lagoudakis, J. Lupton, N. P. Barradas, E. Alves, S. Pereira, I. M. Watson, M. D. Dawson, J. Feldmann, R. Murray, and D. D. C. Bradley, *Efficient dipole-dipole coupling of Mott-Wannier and Frenkel excitons in (Ga,In)N quantum well/polyfluorene semiconductor heterostructures*, Physical Review B **76**, 035344 (2007).
- [5] V. Agranovich, H. Benisty, and C. Weisbuch, *Organic and inorganic quantum wells in a microcavity: Frenkel-Wannier-Mott excitons hybridization and energy transformation*, Solid State Communications **102**, 631 (1997).
- [6] C. Weisbuch, M. Nishioka, A. Ishikawa, and Y. Arakawa, *Observation of the coupled exciton-photon mode splitting in a semiconductor quantum microcavity*, Physical Review Letters **69**, 3314 (1992).
- [7] L. S. Dang, D. Heger, R. André, F. Bœuf, and R. Romestain, *Stimulation of polariton photoluminescence in semiconductor microcavity*, Physical Review Letters **81**, 3920 (1998).
- [8] J. Kasprzak, M. Richard, S. Kundermann, A. Baas, P. Jeambrun, J. M. J. Keeling, F. M. Marchetti, M. H. Szymańska, R. André, J. L. Staehli, V. Savona, P. B. Littlewood, D. B., and L. S. Dang, *Bose – Einstein condensation of exciton polaritons*, Nature **443**, 409 (2006).
- [9] A. Amo, J. Lefrère, S. Pigeon, C. Adrados, C. Ciuti, I. Carusotto, R. Houdré, E. Giacobino, and A. Bramati, *Superfluidity of polaritons in semiconductor microcavities*, Nature Physics **5**, 805 (2009).
- [10] A. Kavokin, J. J. Baumberg, G. Malpuech, and F. P. Laussy, *Microcavities* (Oxford University Press, 2017).
- [11] S. Klemmt, T. Harder, O. Egorov, K. Winkler, R. Ge, M. Bandres, M. Emmerling, L. Worschech, T. Liew, M. Segev, S. C, and S. Höfling, *Exciton-polariton topological insulator*, Nature **562**, 552 (2018).
- [12] P. Stepanov, I. Amelio, J.-G. Rousset, J. Bloch, A. Lemaître, A. Amo, A. Minguzzi, I. Carusotto, and M. Richard, *Dispersion relation of the collective excitations in a resonantly driven polariton fluid*, Nature Communications **10**, 1 (2019).
- [13] X. Zhong, T. Chervy, L. Zhang, A. Thomas, J. George, C. Genet, J. A. Hutchison, and T. W. Ebbesen, *Energy Transfer between Spatially Separated Entangled Molecules*, Angewandte

- Chemie International Edition **56**, 9034 (2017).
- [14] D. M. Coles, N. Somaschi, P. Michetti, C. Clark, P. G. Lagoudakis, P. G. Savvidis, and D. G. Lidzey, *Polariton-mediated energy transfer between organic dyes in a strongly coupled optical microcavity*, Nature Materials **13**, 712 (2014).
- [15] J. Feist and F. J. Garcia-Vidal, *Extraordinary exciton conductance induced by strong coupling*, Physical Review Letters **114**, 196402 (2015).
- [16] X. Zhong, T. Chervy, S. Wang, J. George, A. Thomas, J. A. Hutchison, E. Devaux, C. Genet, and T. W. Ebbesen, *Non-Radiative Energy Transfer Mediated by Hybrid Light-Matter States*, Angewandte Chemie International Edition **55**, 6202 (2016).
- [17] R. Jayaprakash, K. Georgiou, H. Coulthard, A. Askitopoulos, S. K. Rajendran, D. M. Coles, A. J. Musser, J. Clark, I. D. Samuel, G. A. Turnbull, et al., *A hybrid organic-inorganic polariton LED*, Light: Science & Applications **8**, 1 (2019).
- [18] J.-G. Rousset, B. Piętka, M. Król, R. Mirek, K. Lekenta, J. Szczytko, W. Pacuski, and M. Nawrocki, *Magnetic field effect on the lasing threshold of a semimagnetic polariton condensate*, Physical Review B **96**, 125403 (2017).
- [19] D. Caputo, E. Sedov, D. Ballarini, M. Glazov, A. Kavokin, and D. Sanvitto, *Magnetic control of polariton spin transport*, Communications Physics **2**, 1 (2019).
- [20] J. K. Furdyna, *Diluted magnetic semiconductors*, Journal of Applied Physics **64**, R29 (1988).
- [21] J. Sadowski, H. Mariette, A. Wasiela, and Y. M. d'Aubigné, *Multiple quantum well exciton Bragg mirrors, tunable by magnetic field*, Thin Solid Films **306**, 296 (1997).
- [22] G. Panzarini, L. C. Andreani, A. Armitage, D. Baxter, M. S. Skolnick, V. N. Astratov, J. S. Roberts, A. V. Kavokin, M. R. Vladimirova, and M. A. Kaliteevski, *Exciton-light coupling in single and coupled semiconductor microcavities: Polariton dispersion and polarization splitting*, Physical Review B **59**, 5082 (1999).
- [23] S. Richter, T. Michalsky, L. Fricke, C. Sturm, H. Franke, M. Grundmann, and R. Schmidt-Grund, *Maxwell consideration of polaritonic quasi-particle Hamiltonians in multi-level systems*, Applied Physics Letters **107**, 231104 (2015).
- [24] S. Dufferwiel, F. Li, A. A. P. Trichet, L. Giriunas, P. M. Walker, I. Farrer, D. A. Ritchie, J. M. Smith, M. S. Skolnick, and D. N. Krizhanovskii, *Tunable polaritonic molecules in an open microcavity system*, Applied Physics Letters **107**, 201106 (2015).
- [25] R. P. Stanley, R. Houdré, U. Oesterle, M. Ilegems, and C. Weisbuch, *Coupled semiconductor*

- microcavities*, Applied Physics Letters **65**, 2093 (1994).
- [26] A. Armitage, M. S. Skolnick, V. N. Astratov, D. M. Whittaker, G. Panzarini, L. C. Andreani, T. A. Fisher, J. S. Roberts, A. V. Kavokin, M. A. Kaliteevski, and M. R. Vladimirova, *Optically induced splitting of bright excitonic states in coupled quantum microcavities*, Physical Review B **57**, 14877 (1998).
- [27] M. Ściesiek, W. Pacuski, J.-G. Rousset, M. Parlińska-Wojtan, A. Golnik, and J. Suffczyński, *Design and control of mode interaction in coupled ZnTe optical microcavities*, Crystal Growth & Design **17**, 3716 (2017).
- [28] M. Bayindir, C. Kural, and E. Ozbay, *Coupled optical microcavities in one-dimensional photonic bandgap structures*, Journal of Optics A: Pure and Applied Optics **3**, S184 (2001).
- [29] K. Sebald, M. Seyfried, S. Klemmt, S. Bley, A. Rosenauer, D. Hommel, and C. Kruse, *Strong coupling in monolithic microcavities with ZnSe quantum wells*, Applied Physics Letters **100**, 161104 (2012).
- [30] T. Klein, S. Klemmt, E. Durupt, C. Kruse, D. Hommel, and M. Richard, *Polariton lasing in high-quality selenide-based micropillars in the strong coupling regime*, Applied Physics Letters **107**, 071101 (2015).
- [31] J.-G. Rousset, B. Piętka, M. Król, R. Mirek, K. Lekenta, J. Szczytko, J. Borysiuk, J. Suffczyński, T. Kazimierczuk, M. Goryca, T. Smoleński, P. Kossacki, M. Nawrocki, and W. Pacuski, *Strong coupling and polariton lasing in Te based microcavities embedding (Cd,Zn)Te quantum wells*, Applied Physics Letters **107**, 201109 (2015).
- [32] K. Sawicki, J.-G. Rousset, R. Rudniewski, W. Pacuski, M. Ściesiek, T. Kazimierczuk, K. Sobczak, J. Borysiuk, M. Nawrocki, and J. Suffczyński, *Triple threshold lasing from a photonic trap in a Te/Se-based optical microcavity*, Communications Physics **2**, 38 (2019).
- [33] J. J. Hopfield, *Theory of the Contribution of Excitons to the Complex Dielectric Constant of Crystals*, Physical Review **112**, 1555 (1958).
- [34] Q. X. Zhao, M. Oestreich, and N. Magnea, *Electron and hole g-factors in CdTe/CdMgTe quantum wells*, Applied Physics Letters **69**, 3704 (1996).
- [35] J. Gaj, R. Planel, and G. Fishman, *Relation of magneto-optical properties of free excitons to spin alignment of Mn²⁺ ions in Cd_{1-x}Mn_xTe*, Solid State Communications **29**, 435 (1979).
- [36] P. Kossacki, *Optical studies of charged excitons in II VI semiconductor quantum wells*, Journal of Physics: Condensed Matter **15**, R471 (2003).

- [37] M. Muszyński, H. Teisseyre, K. Sobczak, and J. Suffczyński, *Stable charged exciton in a ZnO/(Zn,Mg)O quantum well at near room temperature*, Applied Physics Letters **117**, 033102 (2020).
- [38] J. Fischer, S. Brodbeck, A. V. Chernenko, I. Lederer, A. Rahimi-Iman, M. Amthor, V. D. Kulakovskii, L. Worschech, M. Kamp, M. Durnev, C. Schneider, A. V. Kavokin, and S. Höfling, *Anomalies of a Nonequilibrium Spinor Polariton Condensate in a Magnetic Field*, Physical Review Letters **112**, 093902 (2014).
- [39] C. Sturm, D. Solnyshkov, O. Krebs, A. Lemaître, I. Sagnes, E. Galopin, A. Amo, G. Malpuech, and J. Bloch, *Nonequilibrium polariton condensate in a magnetic field*, Physical Review B **91**, 155130 (2015).
- [40] M. Król, R. Mirek, D. Stephan, K. Lekenta, J.-G. Rousset, W. Pacuski, A. V. Kavokin, M. Matuszewski, J. Szczytko, and B. Piętka, *Giant spin Meissner effect in a nonequilibrium exciton-polariton gas*, Physical Review B **99**, 115318 (2019).
- [41] P. Price, *Two-dimensional electron transport in semiconductor layers. I. Phonon scattering*, Annals of Physics **133**, 217 (1981).
- [42] D. G. Lidzey, D. D. C. Bradley, A. Armitage, S. Walker, and M. S. Skolnick, *Photon-Mediated Hybridization of Frenkel Excitons in Organic Semiconductor Microcavities*, Science **288**, 1620 (2000).
- [43] G. H. Lodden and R. J. Holmes, *Long-Range, Photon-Mediated Exciton Hybridization in an All-Organic, One-Dimensional Photonic Crystal*, Physical Review Letters **109**, 096401 (2012).
- [44] E. Orgiu, J. George, J. Hutchison, E. Devaux, J. Dayen, B. Doudin, F. Stellacci, C. Genet, J. Schachenmayer, C. Genes, G. Pupillo, P. Samori, and T. W. Ebbesen, *Conductivity in organic semiconductors hybridized with the vacuum field*, Nature Materials **14**, 1123 (2015).
- [45] J. Schachenmayer, C. Genes, E. Tignone, and G. Pupillo, *Cavity-Enhanced Transport of Excitons*, Physical Review Letters **114**, 196403 (2015).
- [46] J. Wenus, R. Parashkov, S. Ceccarelli, A. Brehier, J.-S. Lauret, M. S. Skolnick, E. Deleporte, and D. G. Lidzey, *Hybrid organic-inorganic exciton-polaritons in a strongly coupled microcavity*, Physical Review B **74**, 235212 (2006).
- [47] G. Lanty, S. Zhang, J. S. Lauret, E. Deleporte, P. Audebert, S. Bouchoule, X. Lafosse, J. Zuñiga Pérez, F. Semond, D. Lagarde, F. Médard, and J. Leymarie, *Hybrid cavity polaritons in a ZnO-perovskite microcavity*, Physical Review B **84**, 195449 (2011).

- [48] M. Sliotsky, X. Liu, V. M. Menon, and S. R. Forrest, *Room Temperature Frenkel-Wannier-Mott Hybridization of Degenerate Excitons in a Strongly Coupled Microcavity*, Physical Review Letters **112**, 076401 (2014).
- [49] L. C. Flatten, D. M. Coles, Z. He, D. G. Lidzey, R. A. Taylor, J. H. Warner, and J. M. Smith, *Electrically tunable organic-inorganic hybrid polaritons with monolayer WS₂*, Nature Communications **8**, 14097 (2017).
- [50] M. Waldherr, N. Lundt, M. Klaas, S. Betzold, M. Wurdack, V. Baumann, E. Estrecho, A. Nalitov, E. Cherotchenko, H. Cai, E. A. Ostrovskaya, A. V. Kavokin, S. Tongay, S. Klemmt, S. Höfling, and C. Schneider, *Observation of bosonic condensation in a hybrid monolayer MoSe₂-GaAs microcavity*, Nature communications **9**, 3286 (2018).
- [51] M. Albiez, R. Gati, J. Fölling, S. Hunsmann, M. Cristiani, and M. K. Oberthaler, *Direct Observation of Tunneling and Nonlinear Self-Trapping in a Single Bosonic Josephson Junction*, Physical Review Letters **95**, 010402 (2005).
- [52] K. G. Lagoudakis, B. Pietka, M. Wouters, R. André, and B. Deveaud-Plédran, *Coherent Oscillations in an Exciton-Polariton Josephson Junction*, Physical Review Letters **105**, 120403 (2010).
- [53] M. Abbarchi, A. Amo, V. Sala, D. Solnyshkov, H. Flayac, L. Ferrier, I. Sagnes, E. Galopin, A. Lemaitre, G. Malpuech, and J. Bloch, *Macroscopic quantum self-trapping and Josephson oscillations of exciton polaritons*, Nature Physics **9**, 275 (2013).
- [54] T. C. H. Liew and Y. G. Rubo, *Quantum exciton-polariton networks through inverse four-wave mixing*, Physical Review B **97**, 041302 (2018).
- [55] N. G. Berloff, M. Silva, K. Kalinin, A. Askitopoulos, J. D. Töpfer, P. Cilibrizzi, W. Langbein, and P. G. Lagoudakis, *Realizing the classical XY Hamiltonian in polariton simulators*, Nature Materials **16**, 1120 (2017).
- [56] S. Portolan, L. Einkemmer, Z. Vörös, G. Weihs, and P. Rabl, *Generation of hyper-entangled photon pairs in coupled microcavities*, New Journal of Physics **16**, 063030 (2014).
- [57] R. André and L. S. Dang, *Low-temperature refractive indices of Cd_{1-x}Mn_xTe and Cd_{1-y}MgyTe*, Journal of Applied Physics **82**, 5086 (1997).

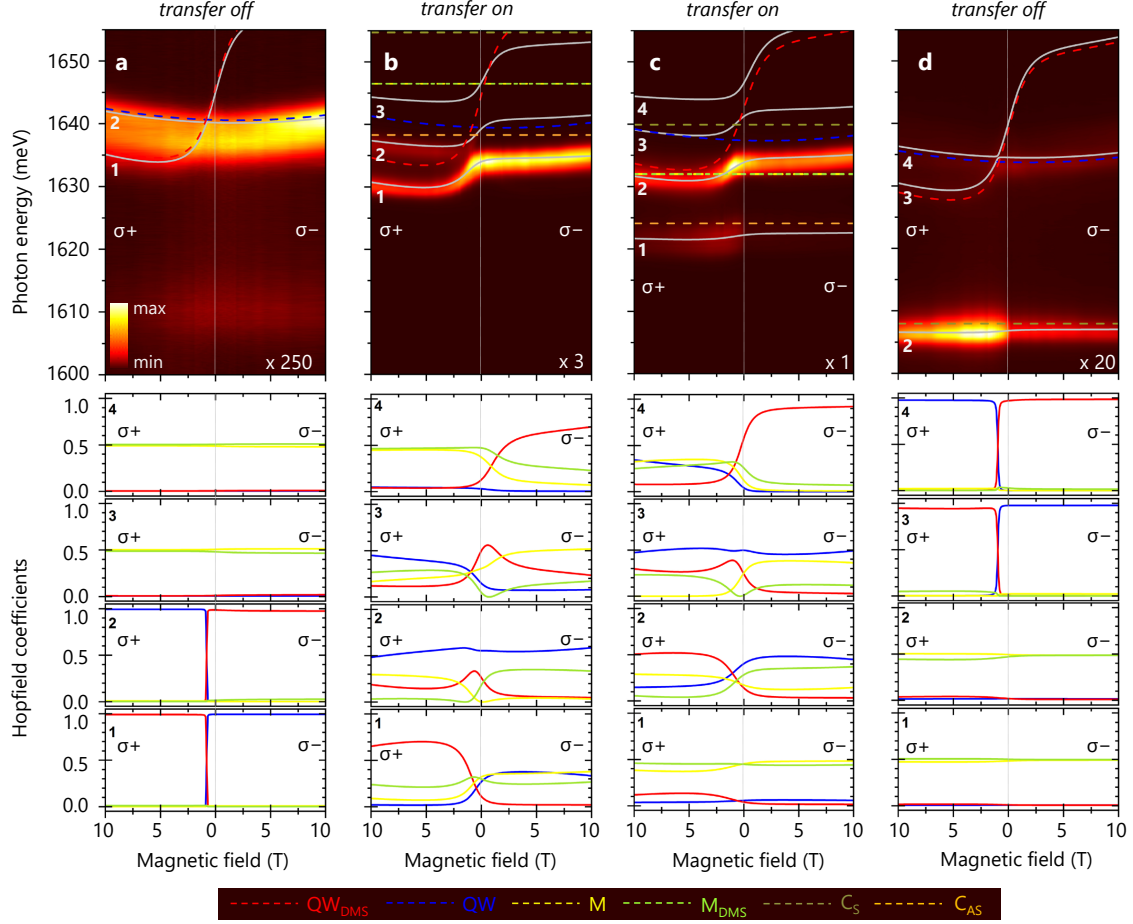


FIG. 4: **Magnetic field controlled, polariton-mediated energy transfer between macroscopically distant quantum wells.** Photoluminescence spectra as a function of the magnetic field for consecutive values of the detuning between the microcavity modes and quantum well excitons, decreasing from **a** to **d**. Circular polarizations of the detection are indicated. The bare levels of the excitons in the QW and QW_{DMS} (simulated following Eq. 2 and 3, respectively), as well as the optical modes M and M_{DMS} of the upper and lower microcavities are shown by the dashed blue, red, yellow, and light-green lines, respectively. Delocalized optical modes C_{AS} and C_S arising from the coupling between M and M_{DMS} are denoted by the dashed orange and olive lines, respectively. Calculated polariton levels are shown by solid white lines. Hopfield coefficients *vs* magnetic field determined in the basis of the QW_{DMS} , QW , M and M_{DMS} for polariton levels from 1 to 4 are provided below the photoluminescence maps with the respective colour code. The "transfer on" case, where the coupled modes are tuned to resonance with the QW and QW_{DMS} excitons enabling long-distance, polariton-mediated energy transfer is shown in panels **b** and **c**. The "transfer off" case, where the coupled modes are detuned with respect to the excitons, which precludes the interaction and energy transfer between magnetic and non-magnetic exciton states is shown in panels **a** and **d**.